Article

JOURNAL OF COMPOSITE MATERIALS

Journal of Composite Materials
2022, Vol. 56(23) 3575–3590

DOI: 10.1177/00219983221114415
journals.sagepub.com/home/jcm
SAGE

Lightweight polyester composites *via* nanoreinforced syntactic foams

Edward DiLoreto[1], Arielle Berman[2], Robert J Moon[3] and Kyriaki Kalaitzidou[1,2]

Abstract

Syntactic foams and their reinforcement with cellulose nanocrystals (CNC) in a thermosetting polyester resin (PR) matrix were studied in order to provide a pathway for lightweight composites for automotive applications with enhanced performance including thermomechanical properties and water uptake. A novel method for coating hollow glass spheres (HGS) with CNC was developed. Various combinations of functionalized CNC and surface modified HGS were studied to determine interactions between the two materials. Surface analysis techniques indicated that CNC were successfully deposited onto the HGS surface and remained at the surface after compounding with PR. Dynamic mechanical analysis of composites samples indicated a 30% increase in high temperature storage modulus between CNC coated HGS samples and uncoated HGS samples. Shifts in tan(δ) peak intensity and beta-relaxation temperature also indicated an increase in interphase volume around CNC coated HGS as compared to uncoated HGS samples. Coating HGS with CNC reduced the maximum water adsorption by as much as 40% indicating the potential for this material system in high moisture environments.

Keywords

composites, nanocellulose, syntactic foams, environmental conditioning

Introduction

Lightweighting, the reduction in density of materials without sacrificing performance using scalable techniques, has been a continuing objective for the field of materials science as it can lead to enhanced fuel efficiency in the transportation sector and thus reduction in greenhouse gas emissions, and increased payload in structural materials. In addition to lightweighting, reduction of the carbon footprint can be achieved by using sustainable or renewable materials. According to theoretical calculations, use of renewable nanomaterials as reinforcements can lead to both lightweighting and sustainable products.[1] However, when it comes to practice the inevitable formation of agglomerates no matter what processing techniques are used limits translation of nanoscale properties to macroscopic structures.[2,3] Furthermore, overall sustainability (i.e. the environmental impact or carbon footprint) of the material system and the resulting product is of growing concern. A common approach to achieving these goals is twofold: reducing the part's mass and incorporating an increased amount of renewable materials.

Cellulose nanomaterials (CNM) are cellulose based nano particles extracted from bulk cellulose materials (e.g. plants, trees, agricultural waste streams, recycled paper, etc.) and can provide mechanical reinforcement to a wide variety of polymers if properly used (e.g. fine-scale dispersion, compatibilizing surface chemistry, etc.). Although CNM mechanical properties are not notably better than other nanomaterials, the biogenic, renewability, biodegradability, low toxicity, and high-volume production potential of these materials makes them particularly appealing.[1,4,5] Additionally, with a density of ~1.59 g/cm^3 the addition of CNM has only a slight effect on the overall composite density. Cellulose nanocrystals (CNC) are one type of CNM and are spindle-shaped particles comprised of highly crystalline cellulose domains. This study will examine the effects of CNC additions to polyester resin (PR) composites. Prior studies demonstrated increased mechanical properties by

[1]School of Materials Science and Engineering,Georgia Institute of Technology, Atlanta, GA, USA
[2]G. W. Woodruff School of Mechanical Engineering,Georgia Institute of Technology, Atlanta, GA, USA
[3]Forest Products Laboratory, U.S. Forest Service, Madison, WI, USA

Corresponding author:
Edward DiLoreto, School of Materials Science and Engineering, Georgia Institute of Technology, North Ave, Atlanta, GA 30332-0002, USA.
Email: etdiloreto@gatech.edu

adding CNCs to glass fiber (GF)-epoxy systems[6,7] and PR resin.[8] Additionally, surface modified CNC-epoxy composites showed increases in glass transition (T_g) by 30°C, tensile strength by 82%, elastic modulus by 21%, and high temperature storage modulus by 160%.[9] In the context of glass fiber reinforced plastic (GFRP) composites the nanoparticles can be either added into the resin paste, into the fiber sizing, or as coating of other fillers.[10]

Syntactic foams, composites that contain hollow spheres in a solid matrix, are widely used in applications that require low density, radiation transparency, or high specific strengths (i.e. automotive body panels, aircraft components, and marine structures). One material used in syntactic foams is hollow glass spheres (HGS) which have low densities (0.2–0.8 g/cm^3) as compared to the conventional GFRP fillers (>1.0 g/cm^3).[11] Substantial property improvements have been reported in syntactic foams by enhancing the interfacial and interphase interactions between the HGS and the matrix through chemical modification or nanoparticle coating.[12,13] To the authors knowledge there has been no work of CNC coating of HGS. Prior work on coating fibers with CNC has shown significant promise.[7] Others have also explored using CNC in conjunction with silanes to enhance surface properties of glass substrates.[14] Translating the processing technology from fibers and planar substrates to HGS will pose a challenge, as is explored in this study.

Extensive research has been conducted in reinforced syntactic foams.[15,16] Various materials including glass and carbon fibers, carbon nanotubes, and clay nanoplatelets have been used in reinforced syntactic foams.[15] These filler materials have shown a general increase in mechanical properties and performance. To the authors knowledge no studies exist that explore the effect of CNC-polymer matrix syntactic foams. Other studies have shown an enhancement in the interface of epoxy-GF when CNC are added to the matrix, indicating the potential for an enhancement of polymer-HGS interface via CNC addition. The Achilles heel of syntactic foams remains the interfacial adhesion strength between the hollow particle and the matrix. Theoretical models and experimental work have confirmed the weakness of the interface.[17] The main method for enhancing interfacial strength is surface modification of the hollow particle via silanes or other chemical agents.[12,18,19] Prior work on coating fibers with CNCs has shown significant promise.[20,21] Others have also explored using CNC in conjunction with silanes to enhance surface properties of glass substrates.[14,20,21] Translating the processing technology from fibers and planar substrates to hollow glass spheres will pose a challenge. Very limited work has been done in the literature on coating hollow particles for syntactic foams with nanomaterials.[22] Thus, translating GF coating technology to HGS surface treatment would greatly expand the property space for syntactic foams.

Syntactic foams of the type investigated in this study i.e. GF and HGS in mixture of unsaturated and vinyl ester resin, are of main interest for automotive applications. The standard SMC composites mainly used currently have a density of 1.7 g/cm^3 and the ultimate goal is to replace those with light weight SMC and ultra-light weight SMC with densities in the range of 1.2–1.4 g/cm^3 and less than 1.0 g/cm^3 respectively that can result in a 30% and more than 40% weight reduction.[23] However, as the amount of HGS is increased the mechanical properties and overall performance including void content and water uptake are compromised. This study focuses on introducing CNCs into the typical syntactic foams in order to address some of these challenges. To isolate the effect GF can have in SMC syntactic foams, this study focuses on the developing a lower density resin formulation which can then be used to make GF SMC composites. Specifically, the role of CNC addition to the matrix polymer and surface modification of HGS (e.g. methacryloxypropyl trimethoxysilane, and/or CNC coatings) in the development of ultra-light weight HGS-PR composites is investigated. The goals of this study are to assess the effects of (1) adding CNC into the PR matrix, (2) varying HGS loading, and (3) coating HGS with CNC on the bulk composite properties.

The novelty of this work is the development of a lightweight polyester resin formulation (syntactic foam) to be used as the resin to make glass fiber sheet molding compounds (SMC) composites for automotive applications. In order to understand the effect of the hollow glass spheres (HGS) on the polyester matrix, no glass fibers were used in this study. This is a polyester resin that is commonly used in SMC automotive composites and the specific HGS used and their surface treatment by 3M are the major candidate material to create syntactic foams for SMC composites.

Materials and methods

Materials

The polyester resin used in this study was a two-part resin, Arotran 774/775 provided courtesy of Ashland Inc. The initiator, methyl ethyl ketone peroxide (MEKP), and the catalyst, cobalt naphthenate (CoNap)-53% in mineral spirits, were purchased from Sigma-Aldrich and Alfa Aesar. Spray dried CNC and never dried CNC 6 wt% aqueous suspensions were purchased from CelluForce.[24] CelluForce CNC are reported to have an individual particle diameter and length of 2.3–4.5 nm and 44–108 nm, respectively, and a sulfate content of 0.246–0.261 mmol/g.[25] The as received spray dried CNC powder consisted of CNC agglomerates having a diameter in the range of 1–50 μm. CNCs which were not surface modified contain sodium counterions and are referred to as NaCNC. Surface modified CNC, Methyl triphenyl phosphoium exchanged CNCs (PhCNC) were produced by Professor Doug Fox from American

University, as described in.[26] PhCNC were supplied in the form of a 4 wt% de-ionized water (DIW) suspension.

Surface treated and untreated HGS were provided by 3M. The surface treated HGS were treated with a 3-(Trimethoxysilyl) propyl methacrylate (<1 wt%) (MS). The HGS are comprised of a soda-lime-borosilicate glass, have a volatile content of 0.5 wt%, a density of 0.32 g/cm^3, and an average diameter of 25 μm with a D95 of 47 μm (95% of the HGS are smaller than 47 μm). These HGS were selected based on the combination of both low density, and good mechanical strength (to minimize damage due to processing and handling).

Composite processing

Some HGS were coated with CNC, following a method similar to that developed by Pacaphol et al.[14] CNC, either NaCNC or PhCNC suspensions, were diluted in DIW at 1 wt% concentration and further dispersed by probe sonication. Sonication was completed with a QSonica Q-500 unit and a ¼" probe, at 40% power (3 s on, 5 s off, for 5 min). Silane treated HGS were then added in a ratio of 10:1 (HGS:CNC) by weight. Ethanol was added to produce a 1:1 ethanol:DIW mixture. The addition of ethanol is necessary to properly disperse the relatively non-polar silane treated HGS. Acetic acid was added to a pH of 4–5 to catalyze the hydrolysis of the silane followed by overnight stirring at ambient temperature and stirring for 2 h at 70°C, after which the mixtures were filtered, rinsed, and dried in an oven at 120°C for 2 h.

Mixtures of spray dried NaCNC with PR were prepared at various ratios by manual mixing followed by probe sonication, QSonica Q-500 with ½" probe, at 50% power alternating 5 s on and 3 s off, in an ice bath, until a target energy density of 500 J/g was reached. Samples were cooled to room temperature at intervals of 2.5 min during sonication. In samples where HGS were added, HGS were mixed manually with the PR until homogeneous. Subsequently, the catalyst, CoNap was added to the mixture at 0.2 wt% and the mixture was stirred. The initiator, MEKP, was then mixed at a ratio of 1.5 wt%. After mixing the system was degassed under vacuum, a small amount was set aside for optical imaging, while the remainder was poured into an open silicone mold, (mold dimensions are identical to those of tensile and dynamic mechanical analysis specimens). Samples were cured at room temperature for 24 h and then post cured at 120°C for 2 h (Figure 1).

Characterization techniques

The quality of the CNC surface coating on the HGS was assessed by X-ray photoelectron spectroscopy (XPS) using a Thermo K-Alpha XPS equipped with a 1.486 KeV aluminum K-alpha X-ray source. Thermogravimetric analysis (TGA) was conducted, using a TA Instruments Q500 TGA, on surface treated HGS to determine the amount of material deposited on the HGS surface through different coating methods. Test specimens of at least 5 mg were heated from 30 to 600°C at a rate of 10°C/min under a Nitrogen atmosphere.

Fracture surfaces and HGS particles were Au/Pd sputter coated for 20–30 s at 0.1 mA using a Cressington 108 sputter coater to reduce charging effects and imaged using a Phenom ProX SEM at 10 kV. Tensile testing was conducted according to ASTM D638 using an Instron 5982 equipped with a 100 kN load cell. A preload of 20 N was applied to remove slack from the load string, and testing was completed using displacement control with a crosshead speed of 5 mm/min.[27] The dogbone neck sample thickness and width were 3.3 mm, and an extensometer MTS-Model-634, with a gauge length of 12.7 mm and an axial travel range of ±10% was used to record the axial strain. Six specimens for each CNC-PR composite type were tested.

Dynamic mechanical analysis (DMA) was used to measure storage and loss modulus, and glass transition temperature (T_g) following ASTM D7028-07[28] and to assess the cumulative effects of the matrix-CNC and/or matrix-HGS interactions (i.e. both chemical interactions such as covalent bonds, and physical interactions such as entanglements) on composite viscoelastic mechanical properties.[29–31] DMA testing was conducted on a TA instruments Q800 DMA using an oscillation of 1 Hz and a heating rate of 5°C/min, ramped from 30 to 250°C. Sample dimensions were 60 mm × 11.9 mm × 3.6 mm, and were tested in 3-pt bending with a span length of 50 mm and a strain of 0.1%. The T_g was defined as the temperature at peak tan(δ). Glassy and rubbery modulus were taken to be the storage modulus at 50°C and 200°C, respectively. At least three specimens per composite type were tested.

The density of the various syntactic foam formulations was determined using water displacement according to ASTM D797-20. The density reported for each formulation is an average of three measurements. Water uptake measurements were conducted in accordance with ASTM D5229.[32] Three DMA bars were used. Samples were dried in an oven at 100°C for 24 h and stored in a desiccator until cooled to room temperature. The testing coupons were aged in 70°C DIW for 1 week. Once per day samples were removed from the water bath, patted dry, and weighed on a balance with precision to 0.1 mg. Samples weighed at least 2 g.

A 95% confidence interval (CI) and Tukey's test was used to determine if mean values were significantly different in test methods where statistical significance is discussed. This method for multiple comparison is useful as it has reduced error over multiple *t*-test comparisons. The method assumes that all observations are independent among

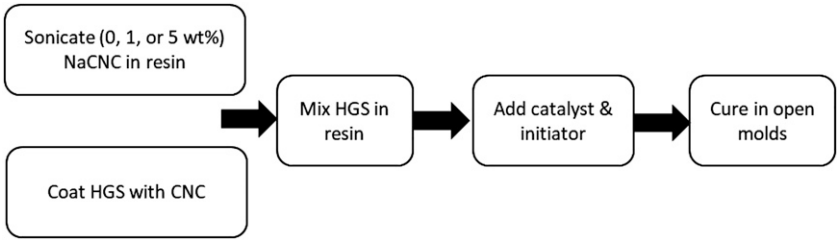

Figure 1. Flowchart of sample manufacturing process.

groups, that the data is normally distributed within a group, and that there is equal within-group variance across all samples.

Experimental outline and sample nomenclature

The naming scheme and composition of each composite are provided in Table 1. Four types of HGS were used: (i) HGS without any surface treatment (HS), (ii) HGS treated with methacryloxypropyl trimethoxysilane (HSMS) (iii) HGS treated with MS and coated with NaCNC referred as HSMSNaCNC, and (iv) HGS treated with MS and coated with PhCNC (HSMSPhCNC). NaCNC were selected as it is one of the most common surface chemistries for CNC while PhCNC have shown to improve the interfacial shear strength over NaCNC coatings.[7,21]

This study investigates (i) What are the interactions between HGS and CNC added either in the resin or as coatings on the HGS and (ii) What are the effects of HGS loading and surface treatment on the properties of the composites. To simplify the discussion, the sample comparisons are divided into three subsets: group I explores interactions between CNC and HGS both added in the resin (i.e. HGS-CNC-PR composites), group II investigates the effect of HGS content and surface treatment with MS, and group III explores the effects of coating HGS with CNC (i.e. CNC coated HGS-PR composites). Samples are named by filler type and amount. For example: 15HS-5NaCNC contains 15 vol% of as received HGS, and 5 wt% spray dried NaCNC, while 15HSMSNaCNC contains 15 vol% of NaCNC coated, MS treated HGS and no spray dried CNC.

Results and discussion

Characterization of surface modified hollow glass spheres

To determine if CNC were successfully coated on the HGS surface various tests were conducted. X-ray photoelectron spectroscopy results presented in Figure 2(a) show that the control HGS sample has some carbon present on the surface near 285 eV. This is likely adventitious carbon but may also be due to a proprietary post treatment of the HGS by the manufacturer. Silane treated HGS (e.g. HSMS) presented an increase in intensity in the 285, 286, and 288 eV, indicating the presence of C-C, C-O, and C=O respectively. These signals reflect the stoichiometric composition of the silane (~5:1:1 for C-C:C-O:C=O).[33] Samples coated with CNCs (e.g. HSMSNaCNC, and HSMSPhCNC) displayed nearly overlapping XPS signals in this range. With the addition of CNC there was a relative increase in C-O intensity as compared to C-C and C=O bonding, based on the stoichiometry of the cellulose monomer (i.e. ~100% C-O).[34]

Thermogravimetric analysis was also used to determine the weight content of the HGS coatings. As shown in Figure 2(b) the weight residue for HS, HSMS, HSMSNaCNC, and HSMSPhCNC samples were 100, 99.2, 98.7, and 95.6 wt%, respectively. The base HS displayed nearly no mass loss in this temperature range as would be expected from a borosilicate soda lime glass material. The silane treated HGS (HSMS) reduces the residue content slightly, and the CNC coatings reduced it further. Interestingly the PhCNC coated sample displayed significantly lower residual mass relative to the NaCNC coated samples, indicating an increased amount of CNC on the surface of HSMSPhCNC samples, or a relatively lower thermal stability of PhCNC than NaCNC. This is consistent with Fox et al. who reported a char yield of 12% for PhCNC and 22% for NaCNC when pyrolyzed under nitrogen.[26] These results are indicative of the presence of less thermally stable material and provide further evidence of surface coating with CNC.

To examine the topographical structure of the coated HGS, SEM imaging was conducted, (Figure 3). The baseline untreated HGS, (Figure 3(a)), have relatively smooth surfaces with only small amounts of electrostatically attached dust. HGS treated with the MS, (Figure 3(b)), had a slightly rougher appearance, likely due to surface inhomogeneities caused by the MS. The silane treated HGS (HSMS) also displayed similar morphology. HGS coated with CNC show film-like surface structures (Figure 3(c) and (d)) but did not show severe agglomeration of HGS particles. Notably, all samples had a minimal number of broken

Table 1. Samples names, filler content and surface modification for samples in this study.

Sample	CNC content (wt%)	HGS content (vol%)	HGS surface modification	Sample Group		
Neat resin	0	0	—	I	II	III
1NaCNC	1	0	—	I		
5NaCNC	5	0	—	I		
15HS	0	15	None	I	II	III
30HS	0	30	None		II	
15HSMS	0	15	MS		II	III
30HSMS	0	30	MS		II	
15HS-1NaCNC	1	15	None	I		
15HS-5NaCNC	5	15	None	I		
15HSMSNaCNC	0	15	MS, NaCNC			III
15HSMSPhCNC	0	15	MS, PhCNC			III

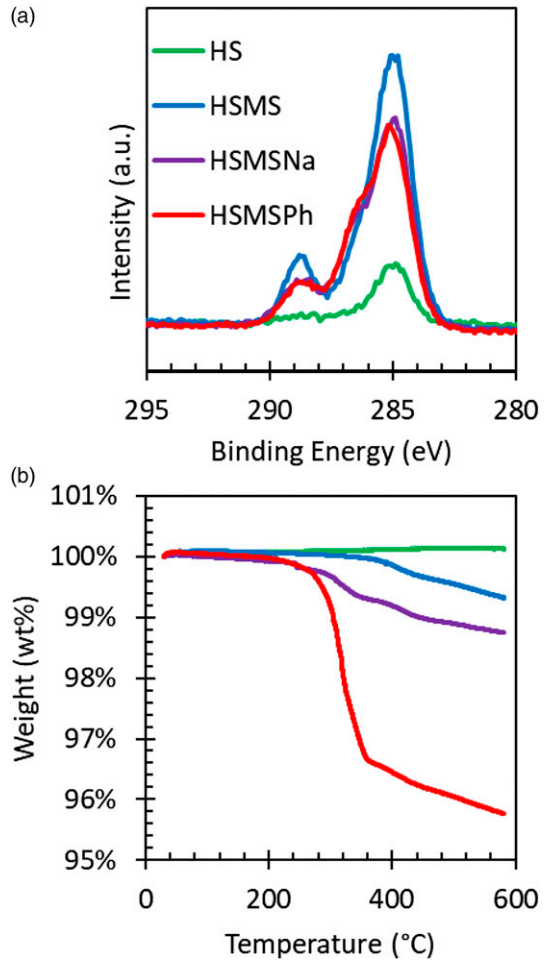

Figure 2. (a) X-ray photoelectron spectroscopy scan of C1s for as prepared hollow glass spheres (before mixing into polyester resin), (b) Thermogravimetric analysis data for various surface modification conditions of hollow glass spheres.

HGS indicating that the surface modification processing did not cause substantial damage.

Although the results do not conclusively indicate that the CNC were covalently bonded to the HGS surface there are several qualitative factors that strongly indicate the presence of CNC-HGS bonding. Initial studies which involved simple mixing of CNC and HGS followed by a DIW rinsing step resulted in no observable CNC on the HGS surface. Considering the hydrophilicity of CNC, any CNC not covalently bonded to the HGS surface are expected to be rinsed away in DIW. Further work is needed to conclusively determine the chemical nature of the CNC-HGS interactions.

Composite mechanical properties

Considering that the amount of HGS is varied between 0 and 30 wt% and of CNC between 0 and 5 wt%, the discussion of the various properties, including the tensile strength and modulus needs to be on the basis of density. The densities of the various formulations investigated in this study are presented in Table 2.

In multi-phase composite structures the tensile modulus is determined by several factors: the elastic modulus of each constituent, the ability for load transfer among constituents, the reinforcement' aspect ratio, and the surface chemistry and structure of each constituent (i.e. interphase effects). There are various studies on PR-CNC and PR-HGS systems but there are no studies on understanding the interactions between CNC and HGS.[4,8,35]

The effects of CNC and HGS when both are added in the resin (i.e., group I: HS, NaCNC, and HS-NaCNC samples) on the tensile modulus and strength of the composite are shown in Figure 4. No surface treatments

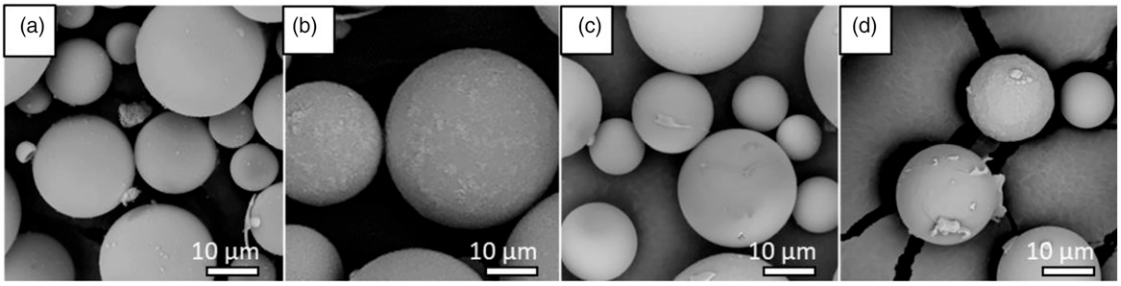

Figure 3. Scanning electron microscopy images of (a) HS, (b) and HSMS, (c) HSMSNaCNC, and (d) HSMSPhCNC.

Table 2. Density of the syntactic foam formulations investigated in this study.

Formulation	Density (g/cm^3)	Standard deviation
Neat resin	1.177	0.002
1NaCNC	1.192	0.003
5NaCNC	1.200	0.001
15HS	1.006	0.001
30HS	0.857	0.003
15HSMS	1.012	0.003
30HSMS	0.861	0.002
15HS-1NaCNC	1.025	0.002
15HS-5NaCNC	1.044	0.001
15HSMSNaCNC	1.023	0.004
15HSMSPhCNC	1.028	0.002

were applied to HGS in this group. The addition of spray dried CNC (1NaCNC, and 5NaCNC) did not significantly (95% confidence level) alter the tensile strength relative to the base polyester whereas the samples with 5 wt% CNC exhibited a significant increase the elastic modulus. Similarly, addition of 15 vol% HGS enhanced the tensile modulus and had no significant effect on the strength, indicating a uniform dispersion of the HGS. The increase in tensile modulus is consistent with previous studies based on the HGS wall thickness and density.[36] The tensile strength values for 15HS-1NaCNC (20.8 MPa) and 15HS-5NaCNC (22.8 MPa) were significantly lower compared to that of the neat resin sample (27.2 MPa). This could possibly be caused by agglomeration of HGS, as the addition of NaCNC into the resin increases the viscosity, which could affect the HGS dispersion during mixing. Hollow glass spheres agglomerates entrapped voids resulting in dry spots acting as areas of stress concentration and leading to decreased strength of the composite. Overall, no significant interaction effects were observed between HGS and NaCNC with respect to tensile strength or elastic modulus as determined by a multiple linear regression analysis (i.e. the regression coefficient was not significantly different from zero at a 95% confidence level).

Considering the increase in modulus by more than 20% when spray dried CNC and HGS are combined, the potential of lightweighting by using syntactic foams becomes apparent as shown in Supplemental Figure S3, where the specific modulus and strength that account for density are plotted. Specifically, 15HS-1NaCNC and 15HS-5NaCNC show an increase in specific tensile modulus of 70% and 25% over their respective CNC-PR composites, with approximately equivalent specific tensile strengths.

The group II samples explored interaction effects between the HGS vol fraction and the HGS surface treatment (Figure 5). In every case the addition of HGS to neat PR resin decreased the average tensile strength of the composite. 15HSMS displayed lower average tensile strength than 15HS, 18 MPa vs 24 MPa (statistically significant at 95% confidence level), probably due to agglomeration of the HGS. The average tensile modulus of 15HSMS was not statistically different than that of 15HS and both samples with 30 vol% HGS had similar tensile strength. The reduced tensile strength in each case is likely due to porosity (see Composite Morphology). The similar tensile strength and observations of entrapped porosity indicate similar failure mechanisms. Tensile strength of syntactic foam composites has been shown to have a positive relationship with density as does the data here.[15] The specific tensile modulus is increased by 38% and 16% for HS and HSMS composites, respectively, upon increasing the HGS content from 15 vol% to 30 vol%. The specific tensile strength is reduced by 39% and 26% for HS and HSMS composites, respectively (Supplemental Figure S3). Although the addition of more HGS has the potential to increase the HGS-PR composite stiffness and specific stiffness the significant reduction in tensile strength was a decisive factor to keep the HGS content to 15 vol% as the benchmark for further testing of surface treated HGS-PR composites. The specific tensile properties for these composites could be improved by further optimization of the process method to eliminate defects including agglomerates and voids; however, such a process optimization study is outside the scope of this work.

The group III samples explored the effect of HGS surface treatments (silane, NaCNC, PhCNC) on composite tensile strength and elastic modulus (Figure 5). As in the previous

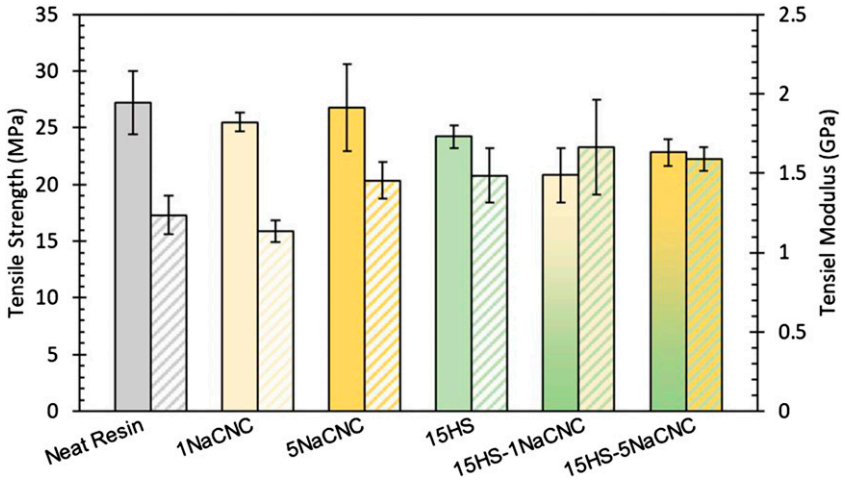

Figure 4. Tensile strength (solid bars) and elastic modulus (patterned bars) as a function of spray dried NaCNC as a reinforcement phase and hollow glass spheres in polyester resin.

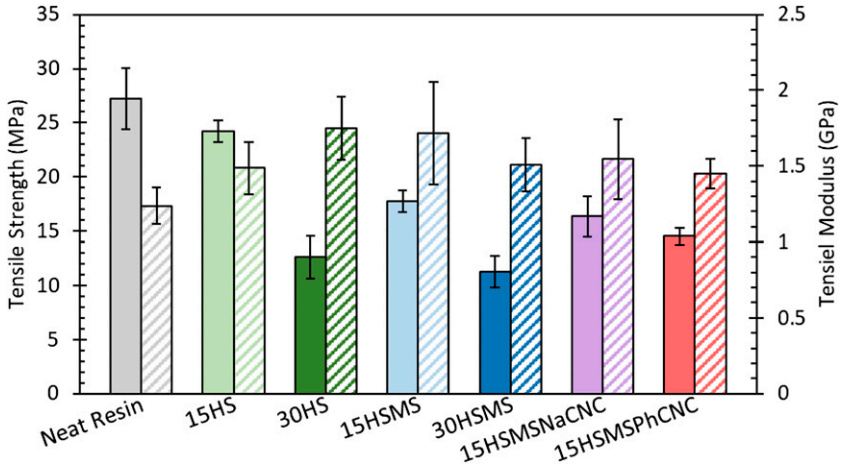

Figure 5. Tensile strength (solid bars) and elastic modulus (patterned bars) for HGS-PR composites with different hollow glass spheres content and various hollow glass spheres surface conditions.

sample group, the addition of HGS to neat PR resin decreased the HGS-PR composite tensile strength in every case. Surface modification of HGS with PhCNC (15HSMSPhCNC) did statistically significantly reduce tensile strength as compared to the 15HSMS case (15 MPa vs 18 MPa). Reduction in tensile strength is considered to result from higher level of HGS agglomeration or an increase in the number of fractured HGS. Tensile modulus measurements showed no significant differences between HGS surface treatments. Only 15HSMS displayed a statistically significant higher modulus from the baseline resin (1.7 vs 1.2 GPa).

The results, despite the large error bars point to the fact that lightweighting is possible considering there is no compromise of the modulus, and in some formulations also of the strength i.e. 15HS while the density is reduced by 14% (see Table 2 and Supplemental Figure S3 in SI documents). Comparing the specific strength to data from the literature the properties observed here are relatively low. Typical values for specific strength and modulus are ~35 MPa mL/g, and ~5 GPa mL/g while this study found values in the range of 12–25 MPa mL/g and 1.0–2.3 GPa mL/g respectively.[15] This is likely due to the reduced base specific properties of the base resin (23 MPa mL/g specific strength and 1.1 GPa mL/g specific modulus).

Composite morphology

Scanning electron microscopy (SEM) was conducted on tensile fracture surfaces to assess the effects on composite

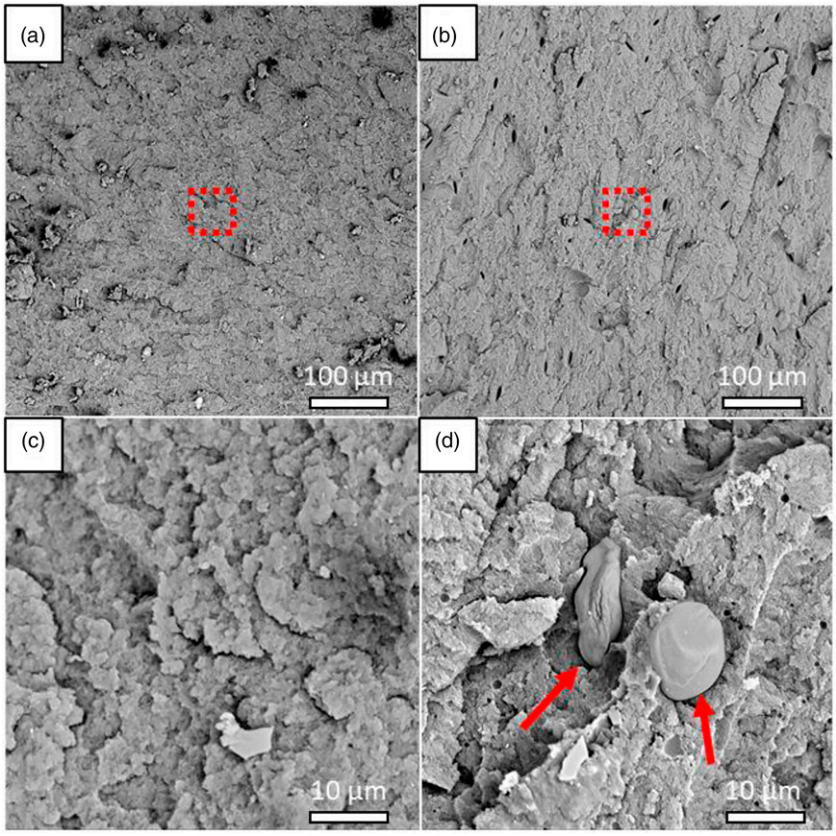

Figure 6. SEM images of the fracture surfaces of neat polyester resin (a and c), and 1NaCNC (b and d). Dotted boxes indicate area of high magnification. Arrows in (d) indicate cellulose nanocrystals aggregates.

microstructure resulting from three mechanisms: (i) CNC and HGS additions to PR matrix, (ii) HGS loadings, and (iii) HGS surface modification.

The effect of CNC and HGS additions on composite microstructure can be assessed by comparing the fracture surfaces of neat PR resin to 1NaCNC and 5NaCNC samples (Figure 6), and to HS (Figure 7). The agglomeration of NaCNC spray dried particles within the PR is immediately evident, having a similar morphology to that of the starting raw sprayed dried material, indicating that the sonication mixing method used in composite processing had minimal effect on redispersing the CNC aggregates. It should be noted that the CNC aggregates seem to be well dispersed. Similar CNC aggregates were also observed and dispersed within 15HS-1NaCNC and 15HS-5NaCNC composite samples (Figure 7). There are solutions to eliminate aggregates but they're very difficult to deal as they involve use of highly toxic or costly solvents and often elevated temperatures that are neither scalable or even if they are scalable they are not attractive to industry. Any wet chemistry or process is not appealing. For example, Kargarzadeh et al.[8] utilize styrene as a reactive solvent to dilute and disperse the CNC into the PR. After full dispersion the excess styrene is boiled off. Such a technique would require significant investment in scaling to prevent release of the highly reactive and carcinogenic styrene monomer.

Failure points were identified in samples containing HGS as either being areas with a high local density of HGS, porosity near the surface, or both (Supplemental Figure S1). The addition of spray dried NaCNC to the PR had no effect on the microstructure, corroborating results from other methods (tensile, DMA, water uptake). The untreated HGS seemed to debond from the matrix cleanly (i.e. a smooth cavity was produced from HGS pullout), indicating a low interfacial energy between HGS and PR (Figures 10). In contrast, the CNC agglomerates appeared to be adhered stronger than HGS to the matrix, indicating they may have had a higher interfacial strength (Figure 7).

The effect of increasing HGS loading from 15 to 30 vol% on the composite microstructure was pronounced. For the 15 vol% HGS samples (both PR, and CNC-PR matrix), the distribution of HGS was uniform with some limited localized accumulation, (Figures 7 and 8). However, by increasing to 30 vol% HGS the localized accumulation of HGS and porosity was more pronounced as indicated by SEM in Supplemental Figure S1. The HGS surface treatment affected the composite microstructure with the MS surface treatment resulting in distinct differences in the HGS

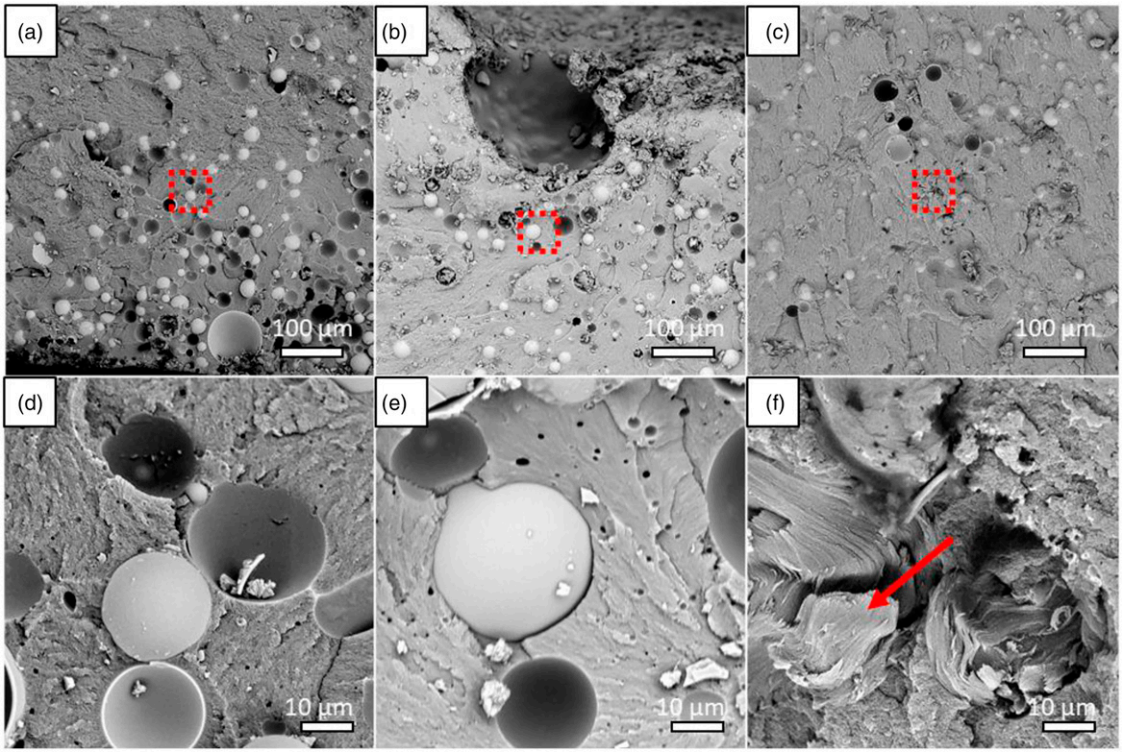

Figure 7. Scanning electron microscopy images of the 15HS (a and d), 15HS-1NaCNC (b and e) and 15HS-5NaCNC (c and f) fracture surfaces. Similar fracture was observed from either matrix resins (neat polyester resin, and NaCNC-PR) where (d) and (e) shows hollow glass spheres-matrix delamination. (f) indicates area where cellulose nanocrystals aggregate was delaminated during fracture. Areas of magnification are denoted by dotted boxes.

pullout cavity morphology as compared to that produced from the as received HGS surface sizing (Figures 7 and 8). The 15HSMS and 30HSMS samples showed noticeably rougher HGS pullout cavities than 15HS and 30HS samples (Figure 7(a) and (d), Figure 8(a) and (d), Supplemental Figure S2(b), (c), (e), and (f)), indicating a higher energy interaction between HGS and PR. The effect of surface treatment on pullout features has been reported in other studies to be related to interfacial shear strength, (i.e. a rougher pullout surface indicated a relatively higher interfacial shear strength).[6,37] Likewise, the CNC coated HGS-PR composite samples, 15HSMSNaCNC and 15HSMSPhCNC, display highly textured HGS pullout surfaces (Figure 8).

Composite thermomechanical properties

Dynamic mechanical analysis (DMA) was conducted to determine the composite materials' performance as a function of temperature and to provide insights into the relaxation behavior of polymer chains in the composite. The relaxation behavior is significantly influenced by the presence of a large volume of interphase which is the case in nano- and micro- composites. The glassy plateau in storage modulus (E′) was not observed as the tests were run at relatively high temperature range due to lack of cooling equipment. Furthermore, at high temperatures the loss modulus decreased to nearly zero. This is believed to be due in part to thermal decomposition of the composite based on observations of discoloration in composites and mass loss of specimens after testing. In case of the Neat Resin, in addition to the primary glass transition, T_g, there is a secondary, beta transition observed in the loss tangent curve centered near ~70°C (T_β). Beta transitions are usually associated with transitions relating to the localized polymer chain or side groups. Its presence here could be indicative of differing relaxation behavior for the main polyester backbone and the interconnecting polystyrene chains.[38] For the sake of discussion, the rubbery modulus is taken at 50°C (E'_g), the glassy modulus at 200°C (E'_r), the T_g as the maximum in the loss tangent, and the maximum of tan(δ) at that transition (I_α). Data is averaged over 3 sample runs.

The group I samples which explore possible interactions between spray dried NaCNC and HGS in the PR matrix are discussed here. There is little difference between the E'_g of the Neat Resin, 1NaCNC, and 15HS samples (Figure 9). The 5NaCNC sample is incrementally higher followed by a step increase to 15HS-1NaCNC and 15HS-5NaCNC. This

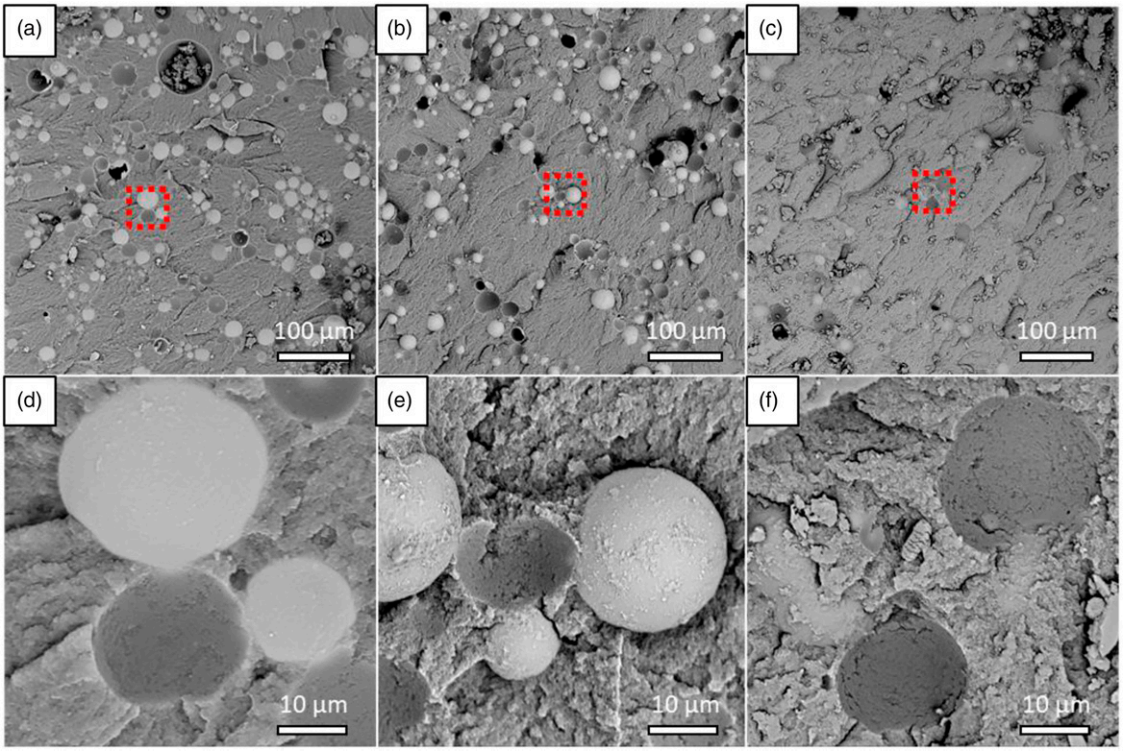

Figure 8. Scanning electron microscopy images of the 15HSMS (a and d), 15HSMSNaCNC (b and e) and 15HSMSPhCNC (c and f) fracture surfaces. Areas of magnification are denoted by dotted boxes.

trend matches, for the most part, the results of the elastic modulus as measured by tensile testing. The main difference being that 15HS is more comparable in modulus to the Neat Resin by DMA than by tensile testing. At elevated temperatures above T_g the difference in E' of the samples are more noticeable. Samples containing HGS, (15HS, 15HS-1NaCNC, 15HS-5NaCNC), display higher E'_r than those without. These effects are easily explained through Halpin-Tsai like concepts on mixtures of materials with differing stiffness. Similar results with respect to CNC-PR composites have been observed in other works.[29,39] The T_g increased from 128.8°C in the Neat Resin to a maximum of 135.9°C in 15HS-1NaCNC and such shifts are often explained via changes in the mobility of polymer chains. In this case it is possible that, although most of the NaCNC is agglomerated, some is nano-dispersed in the resin at this concentration and reducing the polymer free volume. Furthermore, the addition of HGS generally increases the composite rigidity and reduces polymer chain motion. Along with the increase in T_g all samples showed varying degrees of suppression of the beta transition shoulder a possible result of HGS and/or CNC restricting polystyrene side chains in the network.

The group II samples explore the interaction between HGS surface treatment and HGS content (vol%). In order of increasing average E'_g the samples were: Neat Resin, 15HS, 15HSMS, 30HSMS, and 30HS (Figure 10). This trend is somewhat like that observed during tensile testing in that 30HS had both the highest average elastic modulus and E'_r. Both 15HS and 15HSMS E'_g were deemed not statistically significantly different from the Neat Resin sample. At elevated temperature, the E'_r of samples stratified into three distinct tiers: Neat Resin, 15HS and 15HSMS, and 30HS and 30HSMS. Among this sample group the trend seems to indicate that the primary factor driving E'_r is the HGS content. This observation follows with the understanding of each constituent materials performance at elevated temperatures. Glass, having a significantly higher service temperature than PR, would be expected to improve the high temperature stiffness for polymer matrix composites. Examining results in the literature, a similar shift E'_r was observed. Shunmugasamy et al. observed a ~4x increase in E'_r when adding 30 vol% of 0.32 g/cm^3 density HGS to a vinyl ester resin as compared to the neat resin.[40] The T_g of composites was generally increased by further increase of HGS. The MS surface treatment also led to an increase in T_g over untreated samples. Higher HGS loadings also led to a suppression of the beta transition. Higher amounts of HGS material would likely result in further restriction of chain motion and an increase in the activation energy for the transition. The I_α increased with higher HGS content. The I_α is often associated with the interphase volume and

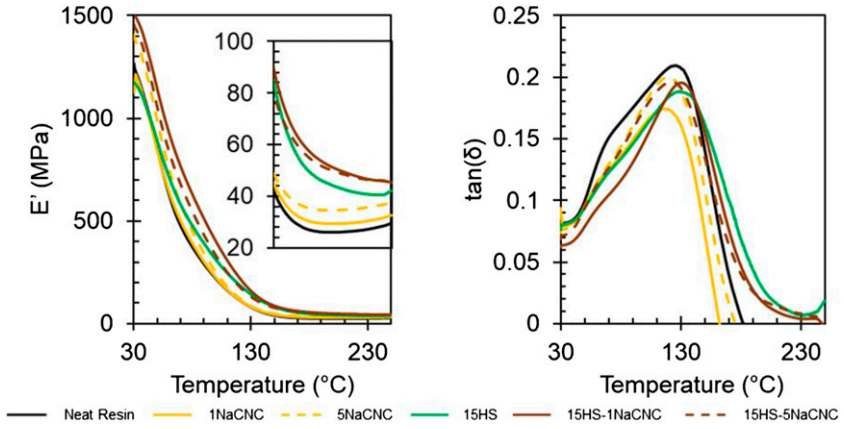

Figure 9. Effect of cellulose nanocrystals content (wt%) on the elastic modulus and tan(δ) of PR, CNC-PR, HGS-PR, and HGS-CNC-PR composites. Insert E′ plot temperature scale projected from main scale.

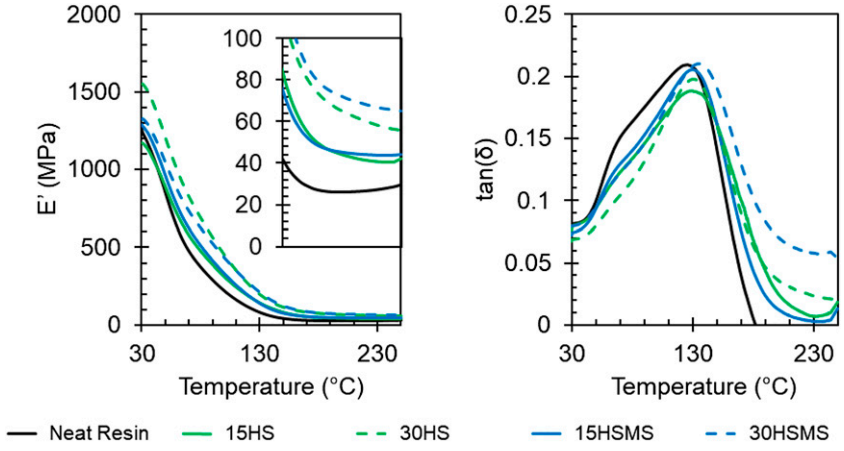

Figure 10. Effect of hollow glass spheres surface treatment and loading on storage modulus and tan(δ) of polyester resin and HGS-PR composites. Insert E′ plot temperature scale projected from main scale.

subsequently the dispersion quality of the fillers. Therefore, the increase in I_α in 30 vol% samples over 15 vol% samples is indicative of possible particle agglomeration. These results show the customizability of syntactic foam composites to specific application requirements. Strong consideration should be taken for surface treatment of the HGS for enhanced bonding as has also been revealed in other studies.[18,41]

The group III samples provided interesting insights into the HGS-PR interphase and the effects of various surface treatments on composite behavior (Figure 11). In order of increasing E'_g the samples were: Neat Resin, 15HS, 15HSMS, 15HSMSNaCNC, and 15HSMSPhCNC. As stated earlier, DMA can provide a more sensitive analysis in the linear elastic strain range than tensile testing. At elevated temperatures the samples, in order of increasing E'_r were: Neat Resin, 15HS, 15HSMS, 15HSMSNaCNC, 15HSMSPhCNC. Interestingly, the 15HSMSPhCNC displayed a statistically significantly higher E'_r than 15HSMS (59.7 MPa vs 45.2 MPa), suggesting that CNC surface coated HGS can outperform covalent crosslinking from the MS treated HGS at elevated temperatures. The similarity between HGS surface treatments in this respect indicates similar effects on polymer chain vibration activation energies. The beta transition observed in the Neat Resin appears to be suppressed somewhat by the addition of the HGS, and further by CNC coated HGS. As mentioned before, this phenomenon is likely related to restriction of smaller vibrational modes in the polymer network. A highly textured particle, such as the CNC coated HGS, could disrupt the styrene linkages within the matrix and increase the T_β. The I_α is lowest in 15HSMSNaCNC samples indicating an increase in the interphase volume relative to other HGS samples. A larger interphase volume could be caused by different degrees of interaction effects between the NaCNC-PR and PhCNC-PR interfaces; however,

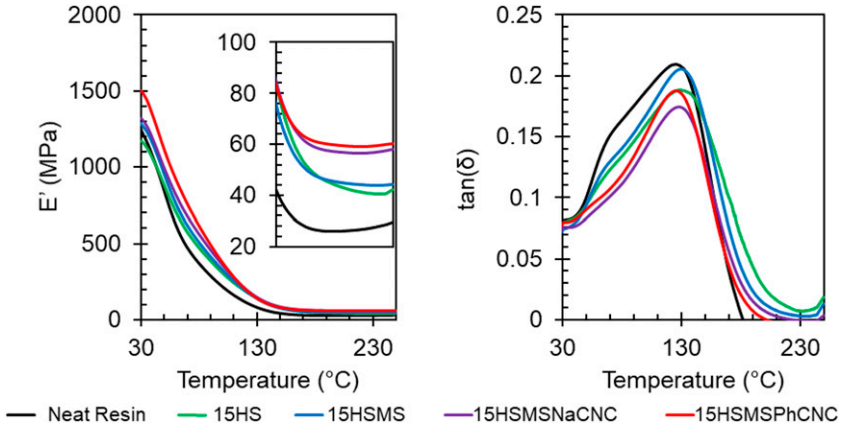

Figure 11. Effect of hollow glass spheres surface treatment on storage modulus and tan(δ) of polyester resin, and HGS-PR composites. Insert E′ plot temperature scale projected from main scale.

considering the tensile strength data the likely cause of this difference is agglomeration of PhCNC coated HGS.

Considered as a whole, the treatment of HGS with CNC produces new effects on the HGS-PR composite behavior that are not observed in HGS-CNC-PR composites, (when CNC is dispersed in the PR resin), including increased E'_r and a reduction of the T_β shoulder. DMA also revealed that PhCNC coated HGS-PR composites at a statistically significantly higher storage modulus than the MS treated HGS-PR composite at high temperature and untreated HGS at lower temperatures. The DMA results outlined here also provide a higher resolution of analysis than was observed via tensile modulus testing, and a more holistic impression than provided by SEM analysis. These DMA results are also generally consistent with the results outlined in previous sections: spray dried NaCNC do not have an interaction effect with HGS, higher levels of HGS loading lead to an increase in stiffness, and surface treatment of HGS with CNC has some effect on HGS-PR interactions.

Composite environmental stability

The environmental stability of the composites was also explored through a water uptake study. Water uptake data is comprised of two primary parameters: apparent diffusivity (D_a), and maximum water uptake (W_{max}). The diffusivity value, taken to be the slope of the initial linear region of the mass uptake versus time$^{1/2}$ plot, is dependent on multiple factors including temperature, pressure or concentration gradients, porosity, and the activation energy for diffusion (e.g. how readily water interacts with components of the material). The W_{max}, is the maximum of the mass gain measurements and is related to the propensity of the material to swell and accept new water molecules, which can be considered to be related to the balance of the chemical potential for water within the composite, and the increased mechanical stress applied for each unit of water absorbed.[42]

Increases in the maximum water uptake value would indicate a composite that would undergo a higher degree of swelling, a higher degree of strain, and subsequently a higher degree of stresses on the composite. Such stresses have often been determined to be detrimental to polymer matrix composite mechanical performance and thus should be minimized.[43,44]

The water uptake behavior of group I samples is shown in Figure 4. Under these environmental conditions the Neat Resin linear region-which is characteristic of the D_a-is brief, completing within 1–2 days of initial submersion. The W_{max} for the Neat Resin is the lowest for all samples studied at 3.3 wt%. This value is within the range reported in similar studies.[45,46] The NaCNC-PR composites displayed higher W_{max} and D_a than the Neat Resin. Considering that most of the CNC particles are likely still agglomerated, this result agrees with results of other studies that have examined water uptake of agglomerated CNMs or micro cellulose polymer matrix composites.[47] The NaCNC agglomerates could provide sites for water to enter and swell the particles that are more readily available and thermodynamically advantageous.[48,49] The HGS-PR composite, 15HS, displayed a substantially higher maximum water uptake over the base resin (9.0 wt% vs 3.3 wt%) and a much clearer linear region. The addition of the high surface area glass particles is the likely source of this dramatic increase. Syntactic foams have been shown to significantly increase the water uptake behavior as compared to the base polymer matrix.[50–52] Glass, being significantly more hydrophilic than PR, has been shown to increase the D_a and W_{max} for PR composites. Adding CNC into the matrix of the HGS-PR composite had a small but noticeable effect on the water uptake behavior (i.e. a W_{max} of 9.5 wt% and 9.0 wt% for 15HS-5NaCNC and 15HS respectively). In the case of 15HS-1NaCNC, the D_a increased somewhat but the W_{max} is still within error of the 15HS sample. The addition of 5 wt% NaCNC (15HS-5NaCNC) both increased the D_a and the

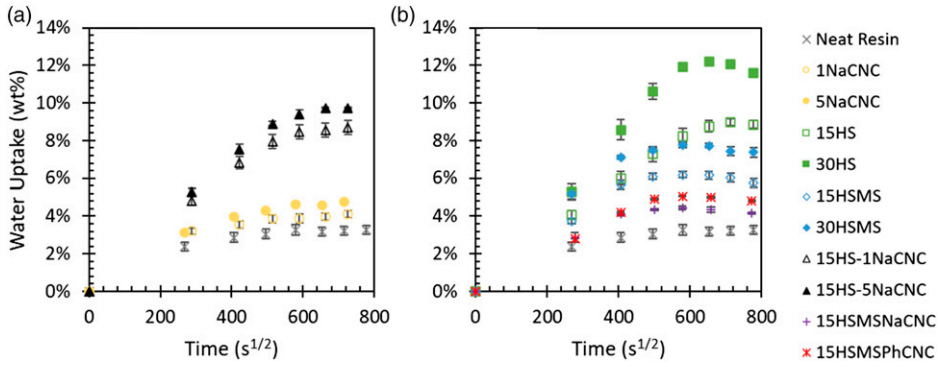

Figure 12. Water uptake for (a) Neat Resin and spray dried NaCNC containing samples, and (b) Neat Resin and HS, HSMS, HSMSNaCNC, and HSMSPhCNC samples.

W_{max}. These results seem to indicate that the presence of the HGS is the dominant mechanism in the water uptake behavior for HGS-PR composites.

The group II samples further reinforce some of the concepts observed within group I (Figure 12(b)), primarily that the high surface area HGS are a dominant driver in HGS-PR composite water uptake behavior. In both the MS treated and untreated HGS case, the presence of more HGS increases the W_{max}. However, the MS silane treatment does significantly reduce the W_{max} between samples with similar HGS content: 31% and 36% for 15 vol% and 30 vol%, respectively. As discussed earlier, the W_{max} is, in part, related to the propensity of the material to swell and accept new water molecules. If the MS treatment of HGS induces crosslinking between the HGS and matrix, as other data in this study and studies elsewhere have suggested, then the polymer immediately surrounding the HGS particles would be more constrained and unable to swell to accept as many water molecules as possible. Interestingly, the D_a is similar among samples with the same content of HGS. This would seem to indicate that the kinetics of water absorption are at least energetically similar (e.g. similar activation energies). Other studies have also found that silane treatment reduces the maximum water uptake by as much as 20% in HGS-epoxy composites with 40 vol% of 60 μm diameter HGS, but also does not significantly change the D_a in the initial region of the water uptake regime. They attribute these differences to the hydrophobic coating formed by the silane around the HGS, thereby limiting the primary mechanism for water ingress into the composite.[52]

The effect of treating HGS with CNC on water uptake behavior is shown in Figure 12(b). The addition of a CNC layer onto the HGS prior to compounding with PR significantly reduced W_{max} and D_a beyond what was observed even in the 15HSMS case and nearly to a level comparable with 5NaCNC. The water uptake curves for 15HSMSNaCNC and 15HSMSPhCNC composites displayed a nearly co-linear D_a in the initial region but separated somewhat in the plateau. The W_{max} for 15HSMSNaCNC and 15HSMSPhCNC composites was 4.4 wt% and 5.1 wt% respectively, averaged over 3 samples. In the initial study by Fox et al. of ion exchanged water adsorption was shown to decrease with functionalization of the relatively hydrophobic methyl triphenyl cation.[26] The W_{max} result is therefore at first perplexing; however, when considering other results from the current study, the likely source of this difference is an increased degree of agglomeration in the PhCNC coated HGS. The over 50% reduction in W_{max} and significant reduction in D_a for CNC coated HGS-PR composites could be connected to the water uptake behavior of nanoparticle thin films. Nanoparticles have been found to reduce the permeability of materials when introduced in a nanodisperse state or as tightly packed thin film coatings. The source of this improved barrier behavior is attributed to the increased tortuosity that many, high aspect ratio particles produce. Furthermore, cellulose films have been shown to have a higher water contact angle than glass, indicating that although both materials would be considered hydrophilic, glass has a higher chemical potential for interaction with water.[48,49] In this study, the CNC are acting as a barrier layer decreasing the availability of the relatively hydrophilic HGS. This finding provides a tremendous opportunity for enhancement in syntactic foams used in underwater environments and perhaps in environments with sustained high humidity.

Conclusions

A framework in the processing of three-phase syntactic foams comprised of polyester resin, hollow glass spheres, and cellulose nanocrystals (CNCs) was reported. The addition of spray dried CNCs into the PR matrix did not have any significant interaction effects with HGS as observed by the methods used here. The presence of HGS at a level of 30 vol% significantly reduced (up to 50%) the tensile strength when compared to similar materials with 15 vol% HGS. Coating HGS with CNCs did not significantly increase the elastic modulus but did increase the storage

modulus both at low temperatures above the base HGS and, at elevated temperatures beyond that of the MS treated HGS composites. Furthermore, coating the HGS with CNC significantly reduced the maximum water uptake and rate of water absorption as compared to samples with untreated HGS or MS treated HGS. The results indicate that CNC coatings on HGS can lead to stronger HGS-matrix interactions. The CNC coating could be influencing mechanical properties through several mechanisms including interpenetration of the resin into the CNC coating increasing the toughness of the interphase and increasing HGS-PR debonding resistance. The reduced water absorbance behavior could be explained by an increase in the tortuosity of the HGS-PR interphase by the CNC coating and by the relatively higher surface energy between CNC and water as compared to that of glass and water.

Addition of CNC coated HGS in PR resulted in composites that exhibited multiscale hierarchical structure and low density able to mitigate some of the detrimental effects of increased HGS loading (i.e. reduction in maximum water uptake). The effect of CNC coating on HGS resulted in increase in elastic modulus and decreased tensile strength compared to those of untreated HGS-PR composites. Measurements taken by DMA provided a clearer distinction between composite types revealing that the PhCNC coated HGS had enhanced performance over the untreated HGS-PR composites both at lower and elevated temperature conditions. Furthermore, a reduction in the T_β peak of the tan(δ) curve indicates the restriction of lower energy rotations of the polymer network upon addition of CNC coated HGS to the PR matrix.

This study provides insights in designing the next generation of syntactic foams to be used as resin in glass fiber/polyester sheet molding compounds (SMC) composites for automotive applications. The density of the SMC composites using syntactic foams as resin is not lowered just because HGS are added to polyester but because the HGS will replace the $CaCO_3$ that has a density of ~2.7 g/cm^3, the heaviest material in SMC that also does not contribute to any property enhancement. $CaCo_3$ is added, among other reasons, to regulate viscosity, eliminate squeeze out during manufacturing of SMC and hot pressing. Considering that these syntactic foams studied here are going to be used as the matrix in SMC composites, the compromised of the mechanical properties of the polyester upon addition of the HGS is acceptable as it can be masked by the reinforcing ability of the GF. In addition, in GF polyester composites both the GF due to their hydrophilic silane sizing and polyester absorb 3%–7% humidity, so the decrease in water uptake due to the addition of HGS is an extra benefit.

Acknowledgements

The authors would also like to acknowledge Dr Satish Kumar at Georgia Tech for providing access to TGA testing equipment. Mechanical testing was completed, in part, at the Materials Properties and Characterization Facility (MPCF) at Georgia Tech by Mr Eric Biederman.

Declaration of Conflicting Interests

The author(s) declared no potential conflicts of interest with respect to the research, authorship, and/or publication of this article.

Funding

The author(s) disclosed receipt of the following financial support for the research, authorship, and/or publication of this article: This work was supported by the P3Nano Grant (Nanocellulose for Lightweight and Low Water Uptake SMC Composites for High Volume Automotive Applications, Grant E18-16). This work was performed in part at the Materials Characterization Facility (MCF) at Georgia Tech. The MCF is jointly supported by the GT Institute for Materials (IMat) and the Institute for Electronics and Nanotechnology (IEN), which is a member of the National Nanotechnology Coordinated Infrastructure supported by the National Science Foundation (Grant ECCS-2025462). This work was also performed in part at the Materials Innovation and Learning Laboratory (MILL) at Georgia Tech.

ORCID iD

Edward DiLoreto https://orcid.org/0000-0002-3921-7982

Supplemental Material

Supplemental material for this article is available online.

References

1. Dhali K, Ghasemlou M, Daver F, et al. A review of nanocellulose as a new material towards environmental sustainability. *Sci Total Environ* 2021; 775: 145871.
2. Vaia RA and Wagner HD. Framework for nanocomposites. *Mater Today* 2004; 7(11): 32–37.
3. Asadi A and Kalaitzidou K. Process-structure-property relationship in polymer nanocomposites. In: Marotti de Sciarra F and Russo P (eds) *Experimental characterization, predictive mechanical and thermal modeling of nanostructures and their polymer composites*. Amsterdam, Netherlands: Elsevier, 2018, pp. 25–100.
4. Kargarzadeh H, Mariano M, Huang J, et al. Recent developments on nanocellulose reinforced polymer nanocomposites: a review. *Polymer* 2017; 132: 368–393.
5. Clarkson CM, El Awad Azrak SM, Forti ES, et al. Recent developments in cellulose nanomaterial composites. *Adv Mater* 2020; 33: 2000718.
6. Asadi A, Miller M, Singh AV, et al. Lightweight sheet molding compound (SMC) composites containing cellulose nanocrystals. *Compos Struct* 2017; 160: 211–219.
7. Haque E, Shariatnia S, Jeong TJ, et al. Scalable coating methods for enhancing glass fiber–epoxy interactions with cellulose nanocrystals. *Cellulose* 2021; 28(8): 4685–4700.

8. Kargarzadeh H, Sheltami RM, Ahmad I, et al. Cellulose nanocrystal: a promising toughening agent for unsaturated polyester nanocomposite. *Polymer* 2015; 56: 346–357.
9. Wang W-J, Wang W-W, Shao Z-Q, et al. Surface modification of cellulose nanowhiskers for application in thermosetting epoxy polymers. *Cellulose* 2014; 21(4): 2529–2538.
10. Orgéas L, Dumont PJ and Nicolais L. Sheet molding compound. In: *Wiley encyclopedia of composites*. Hoboken, NJ: John Wiley & Sons, 2011.
11. Gupta N, Zeltmann SE, Shunmugasamy VC, et al. Applications of polymer matrix syntactic foams. *JOM* 2013; 66(2): 245–254.
12. Li R, Wang P, Zhang P, et al. Surface modification of hollow glass microsphere and its marine-adaptive composites with epoxy resin. *Adv Compos Lett* 2020; 29: 2633366X20974682.
13. Zegeye EF and Woldesenbet E. Processing and mechanical characterization of carbon nanotube reinforced syntactic foams. *J Reinforced Plastics Compos* 2012; 31(15): 1045–1052.
14. Pacaphol K and Aht-Ong D. The influences of silanes on interfacial adhesion and surface properties of nanocellulose film coating on glass and aluminum substrates. *Surf Coat Technol* 2017; 320: 70–81.
15. Gupta N, Pinisetty D and Shunmugasamy VC. *Reinforced polymer matrix syntactic foams: effect of nano and microscale reinforcement*. New York, NY: Springer Science & Business Media, 2013.
16. Paul D, Velmurugan R, Jayaganthan R, et al. Analysis of syntactic foam–GFRP sandwich composites for flexural loads. *J Physics: Conf Series* 2018; 991(1): 012064.
17. Marur PR. Influence of imperfect interface on the elastic moduli of syntactic foams. *Comput Mater Sci* 2009; 46(2): 327–332.
18. Bharath Kumar BR, Doddamani M, Zeltmann SE, et al. Effect of particle surface treatment and blending method on flexural properties of injection-molded cenosphere/HDPE syntactic foams. *J Mater Sci* 2016; 51(8): 3793–3805.
19. Li G and Jones N. Development of rubberized syntactic foam. *Compos A: Appl Sci Manufact* 2007; 38(6): 1483–1492.
20. Asadi A, Miller M, Moon RJ, et al. Improving the interfacial and mechanical properties of short glass fiber/epoxy composites by coating the glass fibers with cellulose nanocrystals. *Express Polym Lett* 2016; 10(7): 587–597.
21. Goswami J, Haque E, Fox DM, et al. The effect of cellulose nanocrystal coatings on the glass fiber-epoxy interphase. *Materials* 2019; 12(12): 1951.
22. Herrera-Ramírez LC, Cano M, de Villoria RG, et al. Low thermal and high electrical conductivity in hollow glass microspheres covered with carbon nanofiber–polymer composites. *Compos Sci Technol* 2017; 151: 211–218.
23. Gregl BV, Larson LD, Sommer M, et al. Formulation advancements in hollow-glass microspheres filled SMC. *J Mater Manufact* 1999; 108: 797–805.
24. CelluForce. Nanocrystalline Cellulose Manufacturing Experts. 2021. Available from: https://www.celluforce.com/en/home/
25. Reid MS, Villalobos M, Cranston ED, et al. Benchmarking cellulose nanocrystals: from the laboratory to industrial production. *Langmuir* 2017; 33(7): 1583–1598.
26. Fox DM, Rodriguez RS, Devilbiss MN, et al. Simultaneously Tailoring surface energies and thermal stabilities of cellulose nanocrystals using ion exchange: effects on polymer composite properties for transportation, infrastructure, and renewable energy applications. *ACS Appl Mater Inter* 2016; 8(40): 27270–27281.
27. ASTM. *Test method for tensile properties of plastics*. West Conshohocken, PA: ASTM International, 2014.
28. ASTM. *Standard test method for glass transition temperature (DMA Tg) of polymer matrix composites by dynamic mechanical analysis (DMA)*. West Conshohocken, PA: ASTM International, 2015.
29. Kargarzadeh H, Sheltami RM, Ahmad I, et al. Toughened polyester cellulose nanocomposites: effects of cellulose nanocrystals and liquid epoxidized natural rubber on morphology and mechanical properties. *Ind Crops Prod* 2015; 72: 125–132.
30. Ferreira JAM, Capela C, Costa JD, et al. Dynamic mechanical analysis of hybrid fibre/glass microspheres composites. *Strain* 2011; 47(3): 275–280.
31. Khoshkava V and Kamal MR. Effect of cellulose nanocrystals (CNC) particle morphology on dispersion and rheological and mechanical properties of polypropylene/CNC nanocomposites. *ACS Appl Mater Inter* 2014; 6(11): 8146–8157.
32. ASTM. *Test method for moisture absorption properties and equilibrium conditioning of polymer matrix composite materials*. West Conshohocken, PA: ASTM International, 2014.
33. Garbassi F, Occhiello E, Bastioli C, et al. A quantitative and qualitative assessment of the bonding of 3-methacryloxypropyltrimethoxysilane to filler surfaces using XPS and SSIMS (FABMS) techniques. *J Colloid Interface Sci* 1987; 117(1): 258–270.
34. Yin Y, Ma J, Tian X, et al. Cellulose nanocrystals functionalized with amino-silane and epoxy-poly (ethylene glycol) for reinforcement and flexibilization of poly (lactic acid): material preparation and compatibility mechanism. *Cellulose* 2018; 25(11): 6447–6463.
35. DiLoreto E, Berman A and Kalaitzidou K. Glass fiber reinforced polyester syntactic foam. In: *American society for composites*. Atlanta, GA: Proceedings of the American Society for Composites—Thirty-fourth Technical Conference, 2019.
36. Porfiri M and Gupta N. Effect of volume fraction and wall thickness on the elastic properties of hollow particle filled composites. *Compos B: Eng* 2009; 40(2): 166–173.
37. Asadi A, Miller M, Sultana S, et al. Introducing cellulose nanocrystals in sheet molding compounds (SMC). *Compos A: Appl Sci Manufact* 2016; 88: 206–215.

38. Menard KP and Menard N. Dynamic mechanical analysis. In: *Encyclopedia of analytical chemistry: applications*. Hoboken, NJ: Theory and Instrumentation, 2006, pp. 1–25.
39. Dufresne A. Dynamic mechanical analysis of the interphase in bacterial polyester/cellulose whiskers natural composites. *Compos Inter* 2012; 7(1): 53–67.
40. Shunmugasamy VC, Pinisetty D, Gupta N, et al. Viscoelastic properties of hollow glass particle filled vinyl ester matrix syntactic foams: effect of temperature and loading frequency. *J Mater Sci* 2013; 48(4): 1685–1701.
41. Deepthi M, Sharma M, Sailaja R, et al. Mechanical and thermal characteristics of high density polyethylene–fly ash cenospheres composites. *Mater Des* 2010; 31(4): 2051–2060.
42. Derrien K and Gilormini P. The effect of applied stresses on the equilibrium moisture content in polymers. *Scripta Materialia* 2007; 56(4): 297–299.
43. Kasturiarachchi KA and Pritchard G. Water absorption of glass/epoxy laminates under bending stresses. *Composites* 1983; 14(3): 244–250.
44. Gupta N and Woldesenbet E. Hygrothermal studies on syntactic foams and compressive strength determination. *Compos Struct* 2003; 61(4): 311–320.
45. Dhakal H, Zhang Z, Richardson M, et al. Effect of water absorption on the mechanical properties of hemp fibre reinforced unsaturated polyester composites. *Compos Sci Technol* 2007; 67(7–8): 1674–1683.
46. Ellis B and Found M. The effects of water absorption on a polyester/chopped strand mat laminate. *Composites* 1983; 14(3): 237–243.
47. Gao C, Wan Y, He F, et al. Mechanical, moisture absorption, and photodegradation behaviors of bacterial cellulose nanofiber- reinforced unsaturated polyester composites. *Adv Polym Technol* 2011; 30(4): 249–256.
48. Chen Y, Zhou X, Yin X, et al. A novel route to modify the interface of glass fiber-reinforced epoxy resin composite via bacterial cellulose. *Int J Polymeric Mater Polymeric Biomater* 2014; 63(4): 221–227.
49. Dankovich TA and Gray DG. Contact angle measurements on smooth nanocrystalline cellulose (I) thin films. *J Adhesion Sci Technol* 2011; 25(6–7): 699–708.
50. Sauvant-Moynot V, Gimenez N, Sautereau H, et al. Hydrolytic ageing of syntactic foams for thermal insulation in deep water: degradation mechanisms and water uptake model. *J Mater Sci* 2006; 41(13): 4047–4054.
51. Grosjean F, Bouchonneau N, Choqueuse D, et al. Comprehensive analyses of syntactic foam behaviour in deepwater environment. *J Mater Sci* 2009; 44(6): 1462–1468.
52. Strauchs A, Mashkin A, Schnettler A, et al. The impact of water absorption on the dielectric properties of syntactic foam. In: *2010 10th IEEE international conference on solid dielectrics*. Potsdam, Germany: IEEE, 2010.